Promotion of Ammonium Formate and Formic Acid Decomposition over Au/TiO2 by Support Basicity under SCR-Relevant Conditions

ARTICLE *in* ACS CATALYSIS · AUGUST 2015

Impact Factor: 9.31 · DOI: 10.1021/acscatal.5b01057

5 AUTHORS, INCLUDING:

Manasa Sridhar

ETH Zurich and Paul Scherrer Institut

6 PUBLICATIONS **8** CITATIONS

SEE PROFILE

Davide Ferri

Paul Scherrer Institut

134 PUBLICATIONS **2,725** CITATIONS

SEE PROFILE

Jeroen A van Bokhoven

ETH Zurich

268 PUBLICATIONS **6,108** CITATIONS

SEE PROFILE

ACS Catalysis

Research Article

pubs.acs.org/acscatalysis

Promotion of Ammonium Formate and Formic Acid Decomposition over Au/TiO_2 by Support Basicity under SCR-Relevant Conditions

Manasa Sridhar,[†,‡] Davide Ferri,[†] Martin Elsener,[†] Jeroen Anton van Bokhoven,[*,†,‡] and Oliver Kröcher[*,†,§]

[†]Paul Scherrer Institut, 5232 Villigen, Switzerland

[‡]ETH Zurich, Institute for Chemical and Bioengineering, 8093 Zurich, Switzerland

[§]École Polytechnique Fédérale de Lausanne (EPFL), Institute of Chemical Sciences and Engineering, 1015 Lausanne, Switzerland

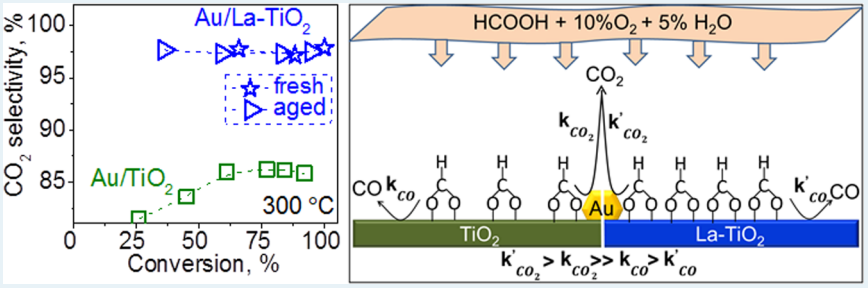

ABSTRACT: This work demonstrates the rational design of a dedicated hydrolysis catalyst for application in the selective catalytic reduction (SCR) of NO_x. Modification of titania by lanthanum prior to gold deposition entailed highly improved catalytic activities for ammonium formate (AmFo) and formic acid decomposition under SCR-relevant conditions stemming from dual phenomena: particle size effect and base effect. Smaller gold particles were stabilized, and there was higher uptake of CO_2 and formic acid, as demonstrated by HAADF-STEM and in situ DRIFT analyses, respectively. The difference in the activities between the lanthanum-modified, unmodified, and tungsten-modified catalysts was implicitly dictated by the formic acid coverage, which was in turn greatly increased in the presence of base. In situ DRIFT studies under reaction conditions identified formate as a relevant reaction intermediate, under reaction conditions. Higher $E_{a,app}$ alongside a higher pre-exponential factor (A), describe an underlying compensation effect originating from the contribution of enthalpy associated with the desorption of the strongly adsorbed formate, which is consistent with the highly negative formic acid orders observed in the case of the lanthanum-modified catalysts. Gold is essential to achieve selectivity to CO_2; its absence yields CO. The introduction of lanthanum to the catalytic system preferentially promoted the CO_2 formation mechanism, enabling complete decomposition of formic acid selectively to CO_2 at significantly lower gold loading and lower contact times, making it a promising candidate for decomposition of formate-based ammonia precursors in the SCR process.

KEYWORDS: *ammonium formate decomposition, formic acid decomposition, effect of lanthanum modification, gold catalysis, kinetic orders, formic acid adsorption, DRIFT*

1. INTRODUCTION

Selective catalytic reduction (SCR) is one of the successful catalyst technologies for reducing diesel NO_x emissions to levels specified by the current emission standards.[1] Ammonia is commonly used as a reducing agent for the abatement of NO_x in waste gases from stationary sources. However, the potentially hazardous handling and storage issues related to compressed or liquefied ammonia renders it unsuitable for use in automobiles. In this context, an aqueous solution of nontoxic urea is commercially applied as an ammonia source in diesel vehicles.[2] However, urea application has several limitations, such as low melting point, low temperature stability, limited durability, and formation of deposits due to incomplete decomposition of urea.[3,4] Therefore, there is growing interest in replacing urea solution with alternative ammonia precursor compounds. Concentrated guanidinium formate, ammonium formate (AmFo), and methanamide solutions are more thermally stable, freeze at lower temperatures, have higher ammonia storage capacity, and decompose more selectively.[5−8] Fast decomposition of the formate ion of these ammonia precursors is desired due to following reasons. On the one hand, it can be expected that the anionic moiety is destabilized and, on the other, formic acid is thus no longer available to form side products such as methanamide and HCN.[3] For a fundamental understanding of the decomposition chemistry of the aforementioned precursors, AmFo can be used as a simple model compound because it contains all the main structural features which influence the activity and selectivity with respect

Received: May 20, 2015
Revised: July 2, 2015
Published: July 2, 2015

DOI: 10.1021/acscatal.5b01057
ACS Catal. 2015, 5, 4772−4782

to ammonia release and side product formation under realistic conditions.[3] In our previous works, we found that Au/TiO_2 is highly active and selective for AmFo decomposition. It also showed an enhanced decomposition activity in the presence of excess ammonia.[9,10] In an effort to rationally optimize the catalyst on the basis of a functional understanding, we have investigated if such a promotional effect of a gas-phase reactant can be converted into a catalytic effect by support modification with basic additives.

Base promotion by alkali and alkaline-earth metals is frequently encountered in heterogeneous catalysis, particularly in water-gas shift (WGS), methanol re-forming reactions, and catalysis by zeolites.[11−13] Panagiotopoulou et al. observed that the presence of sodium and cesium strengthened CO adsorption on Pt/TiO_2 while facilitating hydrogen desorption making them promising candidates for application in WGS.[14] Ribeiro et al. observed an enhancement in the TOF for the low temperature WGS by a factor of ca. 100 and 4 upon addition of sodium to Pt/Al_2O_3 and $Pt/P25\text{-}TiO_2$, respectively.[15] Recently, Ross et al. observed an improved vapor-phase formic acid decomposition rate over Pd/C doped with K.[16] In the context of catalysis over supported gold catalysts, Zhu et al. reported a steady increase in the activity of Au/C for selective alcohol oxidation with molecular oxygen in nonaqueous media upon addition of NaOH up to 1 mol equiv. The higher activities in the presence of base was attributed to the formation of Au−OH, which was speculated to participate in the H abstraction from alcohol.[17] Lanthanum is a known structural and thermal stabilizer that improves sintering resistance and particle dispersion and is an intrinsic activity promoter due to its basic nature. In an earlier work, Jiang et al. showed that lanthanum addition to $CuO/\gamma\text{-}Al_2O_3$ resulted in superior activity for CO and methane oxidation.[18] Borer and Prins also reported on lanthanum-promoted Rh/SiO_2 catalyst for selective CO hydrogenation to methanol.[19] In both the works, addition of lanthanum influenced the surface interaction with the adsorbates leading to improved oxygen-sorption kinetics and increased hydrogen availability at the catalyst interface.

In the current work, we demonstrate that the previously observed promotional effect of the gas-phase basic-reactant (ammonia)[9] on formic acid decomposition over Au/TiO_2 can also be realized as a catalytic effect by the introduction of lanthanum to provide intrinsic basicity to the metal oxide support. Extrapolating this finding to the other end of the spectrum, the inhibiting effect of acidity was verified by tungsten modification of the catalyst. Insights into the connection between formic acid coverages and the catalytic activity are offered.

2. EXPERIMENTAL SECTION

2.1. Catalyst Preparation and Testing. Au/TiO_2 was prepared by a modified incipient wetness impregnation technique.[9,10] Anatase titania (DT51, Crystal Global; BET surface 90 m^2/g, OD_{50} = 1.7 μm) was impregnated with a 0.032 M solution of $HAuCl_4$ (Sigma), calculated on the basis of the desired gold loading and the volume of water equivalent to the pore volume of the support. The sample was aged for 1 h at room temperature. Washing with 1 M aqueous ammonia solution and distilled water, in that order, ensured effective removal of chlorine from the samples (less than 0.07 wt % as estimated by XPS). Calcination was performed at 400 °C for 5 h in air. The acid- and base-modified catalysts were prepared by the aforementioned procedure using commercial supports DT57 and DT52 (Crystal Global), which constituted 10 wt % each of lanthanum oxide and tungsten oxide, respectively, on anatase TiO_2. ICP-OES analysis indicated gold loadings between 0.45 and 0.55% for the acid- and base-modified and unmodified catalysts. The base- and acid-modified gold catalysts obtained after calcination will be henceforth designated as $Au/La\text{-}TiO_2$ and $Au/W\text{-}TiO_2$. $Au/La\text{-}TiO_2$ was also aged at 600 °C in air for 5 h in a static oven and will be hereupon referred to as $Au/La\text{-}TiO_2$-aged. All of the catalysts contained 0.5 wt % gold unless otherwise mentioned.

A pH-adjusted aqueous suspension consisting of the catalyst powder and Ludox AS-40 (Sigma) as a binder was prepared in accordance with the procedure reported previously.[20] The washcoated ceramic cordierite (400 cpsi, Corning) monoliths were dried using a hot gun and then calcined in air at 400 °C for 5 h. In all the experiments the washcoat loading was ca. 2.5 g L^{-1}.

In the experimental setup, 0.05 mL min^{-1} flow of 40 wt % ammonium formate (AmFo, Sigma) solution or 30 wt % formic acid solution in water was pumped using a Shimadzu LC-20 AD HPLC pump and sprayed by means of a nebulizer (e-pond) on the catalyst-coated monolith[21] in a flow of feed gas containing excess oxygen (10 vol %), water (5 vol %), and balance nitrogen to simulate the highly oxidizing conditions observed in automobile exhaust. The compositions of the precursor solutions were chosen so as to produce isoconcentrations of formic acid in the gas phase. The flow rate was set at 750 L h^{-1} in order to realize high GHSVs in the range of 50000−300000 h^{-1}. The cylindrical monolithic catalysts were wrapped with a ceramic fiber mat before being placed inside the reactor in order to prevent bypass of the reactant gas mixture. A stepwise increase in contact time was achieved by adding monoliths of identical dimensions and washcoat loadings along the reactor axis, thus keeping the total catalyst concentration per unit volume constant along the total length of the monolithic stack. The temperatures up- and downstream of the washcoated monolith were controlled using K-type thermocouples. Gaseous reaction products at the reactor outlet were quantified by FTIR spectroscopy (Antaris, Thermo Nicolet).[6] In all of the experiments, the C-balance was closed within an accuracy of ±3% by summing up CO, CO_2, and formic acid. The very low washcoat loadings used in the study resulted in washcoat thicknesses of ∼1 μm (assuming homogeneous washcoat loading), in which case the existence of an internal mass transport regime can be ruled out.[22,23] The Carberry number (η_{ext}DaII) is a good measure for evaluating the external mass transfer limitation. η_{ext}DaII was calculated in the manner described in our past work,[24] taking into account that the diffusivity of formic acid in air at 290 K is 0.129 cm^2 s^{-1}.[25] We found $\eta_{ext}\mathrm{DaII} \ll 0.1$, indicating that the contribution of external mass transfer limitation under the investigated conditions can be disregarded.

Assuming first-order kinetics,[24,26,27] mass-based rate constants were calculated using the formula

$$k_m = -\frac{V^*}{m}\ln(1 - X)$$

where k_m is the masss-based pseudo-first-order rate constant in L g^{-1} s^{-1}, V^* is the volumetric gas flow under reaction conditions in L s^{-1}, m is the catalyst mass (mass of the washcoat present of the monolith) in g, and X is the conversion, given by

DOI: 10.1021/acscatal.5b01057
ACS Catal. 2015, 5, 4772−4782

$$X\ (\%) = \frac{\mathrm{ppm(HCOOH_{in})} - \mathrm{ppm(HCOOH_{out})}}{\mathrm{ppm(HCOOH_{in})}} \times 100$$

The product yield and selectivity are given by

$$Y_{CO_2}\ (\%) = \frac{\mathrm{ppm}(CO_2)}{\mathrm{ppm(HCOOH_{in})}} \times 100$$

$$Y_{CO}\ (\%) = \frac{\mathrm{ppm(CO)}}{\mathrm{ppm(HCOOH_{in})}} \times 100$$

$$S_{CO_2}\ (\%) = \frac{\mathrm{ppm}(CO_2)}{\mathrm{ppm(HCOOH_{in})} - \mathrm{ppm(HCOOH_{out})}} \times 100$$

$$S_{CO_2}\ (\%) = \frac{\mathrm{ppm(CO)}}{\mathrm{ppm(HCOOH_{in})} - \mathrm{ppm(HCOOH_{out})}} \times 100$$

2.2. Characterization. A Micromeritics Tristar 3000 instrument cooled using liquid nitrogen at 77 K was used to perform nitrogen physisorption. All samples were pretreated at 150 °C for 1 h under a continuous flow of nitrogen to remove volatile impurities. The specific surface areas (SSA) were determined using the Brunauer–Emmett–Teller (BET) method. The phase composition was determined by powder X-ray diffraction (XRD) on a D8 Advance Bruker AXS diffractometer with Cu Kα radiation in a 2θ range of 10–70°. The amount of deposited gold was determined by ICP-OES analysis. Scanning transmission electron microscope (STEM) images were obtained on a Hitachi HD-2700 at 200 kV acceleration voltage. The catalyst powders were dispersed in ethanol and deposited onto a perforated carbon–copper grid. The in situ diffuse reflectance infrared Fourier transform (DRIFT) study of CO_2 and formic acid adsorption was conducted using a Bruker Vertex 70 spectrometer equipped with a liquid nitrogen cooled MCT detector and a Praying Mantis mirror accessory (Harrick). Prior to each CO_2/formic acid adsorption experiment, the sample was first pretreated at 400 °C for 0.5 h under a flow of nitrogen containing 10 vol % oxygen and 5 vol % water in order to remove any carbonate residues that may be present on the catalyst surface. Then, the sample was cooled to 200 °C under flowing nitrogen, at which point the background spectrum was collected in flowing nitrogen. The adsorption experiments were carried out in a homemade in situ cell with a flat CaF_2 window at a total flow rate of 50 mL min^{-1}. The adsorption conditions were controlled as follows: 1000 ppm of CO_2 or 1120 ppm formic acid in nitrogen was flowed over the sample for 15 min and the spectra were recorded by accumulating 100 scans at 4 cm^{-1} resolution and a scanner velocity of 80 kHz. Additionally, an operando-DRIFT study of formic acid adsorption under reaction conditions on the unmodified and lanthanum-modified catalysts was performed. The adsorption conditions were identical to those above except for the feed, which additionally contained 10 vol % oxygen and 5 vol % water, and the background spectrum was collected in this feed.

3. RESULTS AND DISCUSSION

3.1. Catalyst Characterization. The XRD patterns of Au/TiO_2, Au/La-TiO_2, Au/W-TiO_2, and Au/La-TiO_2-aged revealed no reflections corresponding to gold, lanthanum, tungsten, or any other mixed oxide, suggesting that the gold and the additives may be present in a well-dispersed form (Figure 1). Modification by lanthanum and tungsten did not cause shifts of titania reflections, indicating that, if present, introduction of these elements into the titania lattice is rather small. Owing to the large difference in the sizes of La^{3+} (0.115 nm) and Ti^{4+} (0.068 nm), there is very little probability of La^{3+} entering into the lattice structure of titania; however, insertion into the interstitial space can be expected.[28] On the other hand, in the case of gold and tungsten, in addition to the formation of surface-bound species, partial incorporation into the lattice induced by high-temperature calcination may not be ruled out.[29,30] While the average anatase crystallite size is 25 nm in the case of Au/TiO_2, the growth of anatase crystallites is restrained to 11.6 and 11.5 nm for Au/La-TiO_2 and Au/W-TiO_2, respectively. Such an inhibition of the crystal growth of titania upon lanthanum or tungsten modification occurs because they occupy the defect sites which are involved in the particle growth and phase transformation.[28,31] The thermal treatment did not structurally modify the support apart from a modest growth in anatase crystallite size from 11.6 to 14 nm. The BET surface areas of Au/La-TiO_2 and Au/W-TiO_2 are 105 and 90 $m^2\ g^{-1}$, respectively, while those for Au/TiO_2 and Au/La-TiO_2-aged were 78 and 81 $m^2\ g^{-1}$, respectively.

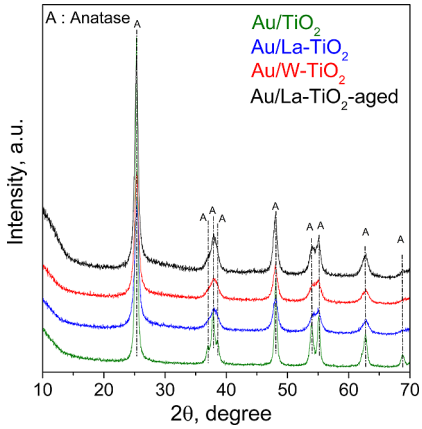

Figure 1. XRD patterns of Au/TiO_2, Au/La-TiO_2, Au/W-TiO_2, and Au/La-TiO_2-aged.

An in situ DRIFT study of CO_2 adsorption was performed to investigate the surface properties of the acid- and base-modified (fresh and aged) and unmodified catalysts. Figure 2a compares the in situ DRIFT spectra obtained after 15 min of contact between the samples and 1000 ppm of CO_2 under a nitrogen flow at 200 °C. CO_2 adsorption on the unmodified and base-modified catalysts resulted in the formation of broad bands between 1600 and 1290 cm^{-1} corresponding to unidentate and bidentate carbonate species,[32−34] while the acid-modified catalyst showed negligible adsorption. Bands centered around 1534 and 1421 cm^{-1} can be assigned to the ν_{as}(OCO) and ν_s(OCO) stretching modes of bidentate bicarbonate species.[35] The lower frequency signals centered around 1570 and 1350 cm^{-1} can arise from monodentate carbonate species. The high intensity of carbonate signals on the base-modified samples confirmed higher CO_2 uptake and thus an increased basicity relative to the other samples. An enhancement in the intensity of bands associated with different carbonate species was observed on the gold-loaded samples in comparison to their bare-support counterparts. The DRIFT spectra of adsorbed

DOI: 10.1021/acscatal.5b01057
ACS Catal. 2015, 5, 4772−4782

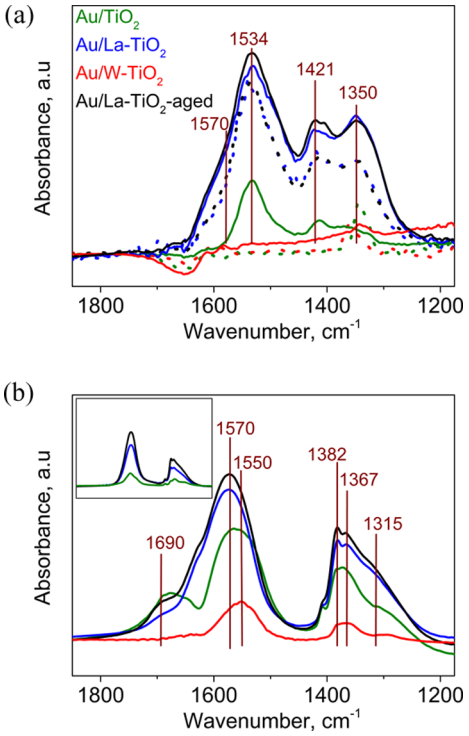

Figure 2. In situ DRIFT spectra of (a) 1000 ppm of CO_2 adsorbed on Au/TiO_2, $Au/La\text{-}TiO_2$, $Au/W\text{-}TiO_2$, and $Au/La\text{-}TiO_2$-aged and their corresponding supports (dotted lines) at 200 °C and (b) 1120 ppm formic acid adsorbed on Au/TiO_2, $Au/La\text{-}TiO_2$, $Au/W\text{-}TiO_2$, and $Au/La\text{-}TiO_2$-aged at 200 °C. Inset: operando DRIFT spectra in the presence of 10% oxygen and 5% water in the same energy range (proportional scales).

CO_2 on $Au/La\text{-}TiO_2$-aged remained practically the same as those on $Au/La\text{-}TiO_2$, indicating that the thermal treatment does not modify the surface basicity of the lanthanum-modified catalyst. The acid-modified samples showed very weak bands, indicating low affinity toward CO_2. Complementary to the CO_2 adsorption studies, the extent of interaction between formic acid and the gold catalysts was also explored.

The in situ DRIFT spectra obtained after 15 min of contact between the catalysts and 1120 ppm of formic acid under a nitrogen flow at 200 °C are presented in Figure 2b. The spectra of the unmodified and base-modified catalysts are characterized by intense signals in the region 1600−1300 cm^{-1} that are associated with the $\nu_{as}(OCO)$ and $\nu_{s}(OCO)$ stretching modes of carboxyl groups of adsorbed formates.[36] Various shoulders on both signals indicate multiple adsorption geometries, namely mono- and bidentate and bridged configurations. The bands at 1690 and 1315 cm^{-1} may originate from monodentate formate species.[37] The high-frequency region (not shown) is also populated by characteristic signals of formate species at 2954, 2867, and 2731 cm^{-1} corresponding to the combination band $\nu_{as}(OCO) + \delta$ (CH), ν(C−H), and the 2δ(CH) overtone, respectively. It is evident that the overall intensity of signals on the base-modified catalysts is larger than that obtained on Au/TiO_2, reflecting higher surface coverage of formate species. In line with the CO_2 adsorption results, there was no significant change in the overall density and position of the adsorbed formate species in the in situ DRIFT spectra after the thermal treatment of $Au/La\text{-}TiO_2$, suggesting closely similar formic acid coverages on both the fresh and the aged base-modified catalysts. The acid-modified catalyst showed the weakest signals associated with formic acid adsorption. In order to observe the surface species under reaction conditions, formic acid adsorption was performed in the presence of 10 vol % oxygen and 5 vol % water and balance nitrogen, simulating the catalytic tests (Figure 2b, inset, proportional *XY* scales). Clearly, the base-modified catalysts (both fresh and aged) exhibited the highest coverage of formate species under the reaction conditions. It is generally accepted that formate is the stable intermediate resulting from the first step in the formic acid decomposition mechanism on most oxide surfaces.[38] Osawa and co-workers employed surface-enhanced infrared adsorption spectroscopy (SEIRAS) and determined that formates adsorbed via two oxygen atoms are the reactive intermediates during formic acid oxidation over a Pt electrode.[39] Similarly, in our case, it is reasonable that a formate-based reactive intermediate participates in the decomposition mechanism.

The HAADF-STEM images of the three catalysts are presented in Figure 3. Lanthanum modification of the support

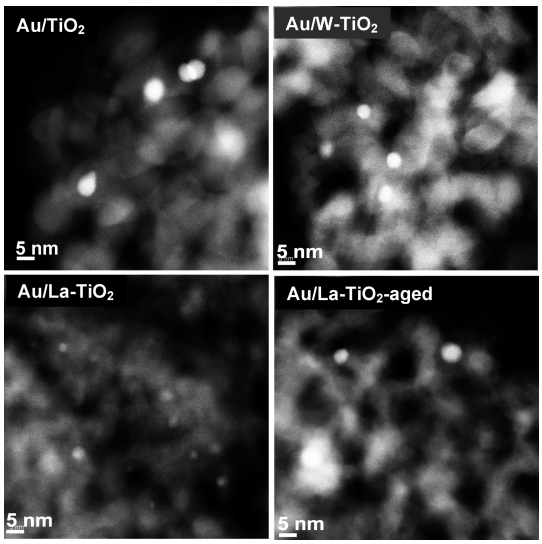

Figure 3. HAADF-STEM images of Au/TiO_2, $Au/W\text{-}TiO_2$, $Au/La_2\text{-}TiO_2$, and $Au/La_2\text{-}TiO_2$-aged.

led to the formation of smaller gold particles in the size range of 2−4 nm, while the unmodified and acid-modified catalysts possessed similar gold particle sizes in the range of 5−7 nm. The structural effect causing stabilization of smaller gold particles on the support upon modification with rare-earth-metal oxides was reported by Ma and co-workers.[40] Yu et al. also reported the formation of smaller gold particles on lanthanum-modified titania due to the possible presence of a large number of defects, such as oxygen vacancies, together with steps and adatoms on which gold immobilization could easily take place.[41] Thermal aging of $Au/La\text{-}TiO_2$ resulted in the growth of gold particles in the size range of those of Au/TiO_2.

3.2. Activity for Ammonium Formate and Formic Acid Decomposition. Au/TiO_2, $Au/La\text{-}TiO_2$, $Au/W\text{-}TiO_2$, and $Au/La\text{-}TiO_2$-aged were tested for ammonium formate (AmFo) and formic acid decomposition in a simulated exhaust gas containing 10 vol % oxygen and 5 vol % water at different temperatures in the range 160−300 °C using various contact times (2.4×10^{-5} g s $cm^{-3} \leq W/F \leq 1.6 \times 10^{-4}$ g s cm^{-3}) (Figure 4a). These catalysts at identical gold loadings differ either by support modification at equal gold particle size (Au/

DOI: 10.1021/acscatal.5b01057
ACS Catal. 2015, 5, 4772−4782

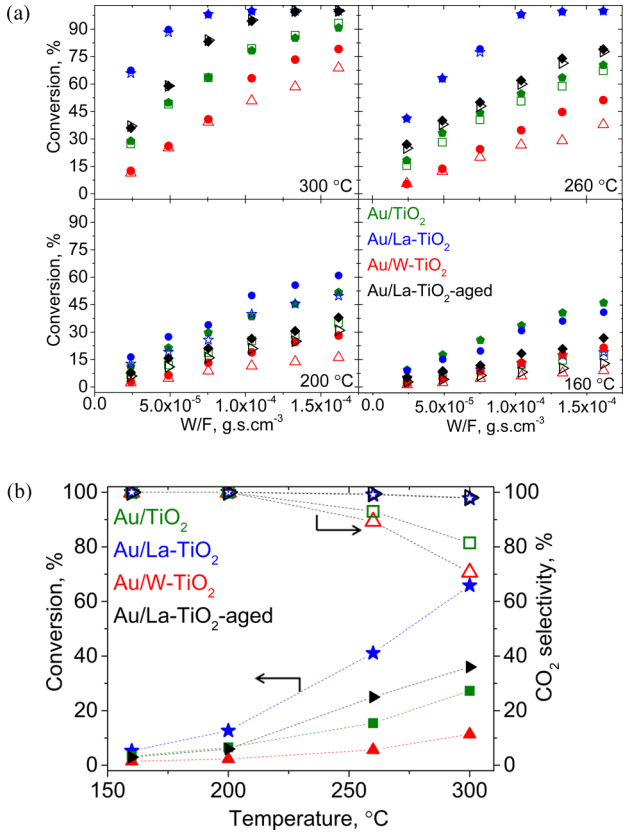

Figure 4. (a) Formic acid conversion as a function of contact time, expressed as W/F (g s cm^{-3}), obtained over Au/TiO$_2$, Au/W-TiO$_2$, Au/La-TiO$_2$, and Au/La-TiO$_2$-aged using AmFo (filled symbols) and formic acid (open symbols) at different temperatures. (b) Temperature dependence of formic acid conversion (filled symbols) and CO$_2$ selectivity (open symbols) over Au/TiO$_2$, Au/W-TiO$_2$, Au/La-TiO$_2$, and Au/La-TiO$_2$-aged at W/F = 2.4 × 10^{-5} g s cm^{-3}.

TiO$_2$ versus Au/W-TiO$_2$ versus Au/La-TiO$_2$-aged) or by gold particle size on the same support (Au/La-TiO$_2$ versus Au/La-TiO$_2$-aged). In agreement with our previous studies,[9] the formic acid conversions obtained at 300 °C over all of the catalysts were identical for formic acid and AmFo. Ammonia was never oxidized. Clearly, at temperatures ≥260 °C, the lanthanum-modified catalysts, both fresh and aged, exhibited higher formic acid conversion, while Au/W-TiO$_2$ showed the lowest performance. Additionally, at these temperatures, the formic acid conversion obtained over the lanthanum-modified catalysts using formic acid as the precursor surpassed the corresponding values obtained over Au/TiO$_2$ using AmFo as the precursor. This observation implies that the promotional effect initiated by base modification surpasses the rate enhancement originating from the presence of a stoichiometric amount of ammonia in the feed gas.[9] At 300 °C, when formic acid was used as the precursor, Au/La-TiO$_2$ and Au/La-TiO$_2$-aged exhibited close to 100% conversion at W/F = 7.5 × 10^{-5} and 1 × 10^{-4} g s cm^{-3}, respectively. In contrast, even at the highest contact time (W/F = 1.6 × 10^{-4} g s cm^{-3}), Au/TiO$_2$ and Au/W-TiO$_2$ did not completely decompose formic acid, resulting in 92% and 69% conversion, respectively. Using the lowest contact time (W/F = 2.4 × 10^{-5} g s cm^{-3}), the formic acid conversion obtained over the unmodified catalyst was <50% of that of Au/La-TiO$_2$ and more than twice that of Au/W-TiO$_2$. Under these conditions, Au/La-TiO$_2$-aged still retained close to 60% of its original activity, thus outperforming the fresh unmodified catalyst. At 260 °C and $W/F \geq 1 \times 10^{-4}$ g s cm^{-3}, the formic acid conversion obtained over Au/La-TiO$_2$ using AmFo and formic acid as precursors reached close to 100% and any further increase in the contact time only led to increased CO$_2$ selectivity. Au/La-TiO$_2$-aged suffered a decrease in conversion owing to the thermal treatment, reaching ∼80% conversion at the highest contact time, still exceeding the performance of Au/TiO$_2$ by more than 15%. At 200 °C, when AmFo was used as the precursor, the formic acid conversion ranged from 70% over Au/La-TiO$_2$ to 50% and 28% over Au/TiO$_2$ and Au/W-TiO$_2$, respectively. At lower temperatures (≤200 °C), the difference in the activities of the unmodified and base-modified catalysts decreased when formic acid was used as the precursor and even turned in favor of the unmodified catalyst when AmFo was used as the precursor. This has two implications: (i) base modification does not improve the formic acid decomposition activity at lower temperatures (≤200 °C), and (ii) the promotional effects derived from the gas-phase and the base modification of the catalyst operate in complementary temperature regimes and, at lower temperatures, the ammonia-induced rate enhancement[9] dominates. While the interaction of ammonia is more favored at lower temperatures,[9] the catalytic effect prevails predominantly at higher temperatures (≥260 °C), which reconciles with the higher $E_{a,app}$ values stemming from the highly negative formic acid orders observed over the base-modified catalysts (see section 3.3). Under all the tested conditions, the acid-modified catalyst was the worst-performing catalyst.

Figure 4b depicts the temperature dependence of formic acid conversion and CO$_2$ selectivity over Au/TiO$_2$, Au/La-TiO$_2$, Au/W-TiO$_2$, and Au/La-TiO$_2$-aged at W/F = 2.4 × 10^{-5} g s cm^{-3}. A progressive drop in CO$_2$ selectivity was evidenced over all the catalysts above 200 °C, with CO being the only other (undesired) product of formic acid decomposition. Evidently, the low activity of the acid-modified catalyst is accompanied by the lowest CO$_2$ selectivity in comparison to the unmodified or base-modified catalysts. The thermal aging at 600 °C did not diminish the CO$_2$ selectivity, which remained >98% in the entire temperature window. At 300 °C, Au/TiO$_2$ exhibited 81% CO$_2$ selectivity, while for Au/W-TiO$_2$ the selectivity is only 70%. At temperatures ≤200 °C, there was no CO production over any of the catalysts. Figure 5a compares the effect of support modification on the CO$_2$/CO ratio at 300 and 260 °C at different contact times. The CO$_2$/CO ratios observed with lanthanum modification remained practically unaffected with aging. There was a striking enrichment of CO$_2$ in the product gas, while the CO formation remained suppressed over the base-modified catalysts. At the two temperatures and W/F = 2.4 × 10^{-5} g s cm^{-3}, the CO$_2$/CO ratio experienced a ∼10-fold increase upon base modification, while acid modification decreased the ratio by 50%. Hence, base modification of the catalyst selectively promotes formic acid decomposition to CO$_2$, reminiscent of the effect of ammonia.[9] Figure 5b compares the CO$_2$ selectivity versus formic acid conversion obtained using formic acid at 300 °C over Au/TiO$_2$, Au/La-TiO$_2$, Au/W-TiO$_2$, and Au/La-TiO$_2$-aged. The base- and acid-modified catalysts exhibited the highest and the lowest CO$_2$ selectivities, respectively, over the whole conversion range. At all contact times, the CO$_2$ selectivity was >98% for the base-modified catalysts, while it dropped to 80% and 70% over Au/TiO$_2$ and Au/W-TiO$_2$, respectively, at W/F = 2.4 × 10^{-5} g s cm^{-3}. The shaded region shows that, at similar conversion

DOI: 10.1021/acscatal.5b01057
ACS Catal. 2015, 5, 4772−4782

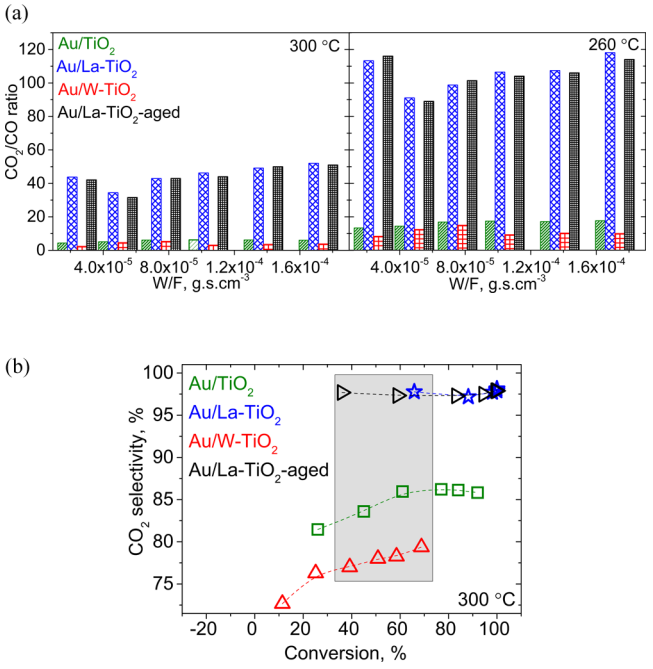

Figure 5. (a) Evolution of CO_2/CO ratio as a function of contact time obtained from formic acid decomposition over Au/TiO_2, $Au/W\text{-}TiO_2$, $Au/La\text{-}TiO_2$, and $Au/La\text{-}TiO_2$-aged at 300 and 260 °C. (b) Formic acid conversion versus CO_2 selectivity obtained over Au/TiO_2, $Au/W\text{-}TiO_2$, $Au/La\text{-}TiO_2$, and $Au/La\text{-}TiO_2$-aged at 300 °C.

levels over the four catalysts, a marked difference exists in the CO_2 selectivity. This strongly suggests that base modification increases the intrinsic propensity to produce CO_2 from formic acid decomposition.

Instead of direct formic acid oxidation to CO_2, formic acid could alternatively first decompose to CO as an intermediate, which subsequently oxidizes to CO_2.[42,43] Gas-phase CO oxidation experiments were performed to assess the contribution of this reaction pathway toward increased CO_2 production from formic acid decomposition over the base-modified catalysts. Figure 6a plots CO conversion as a function of temperature over the fresh and aged base-modified catalysts in the presence and absence of water at $W/F = 1.6 \times 10^{-4}$ g s cm^{-3}. The presence of water adversely affected CO conversion. Under realistic conditions involving 10 vol % water, the CO conversion over both the fresh and aged base-modified catalysts was 50% of those when no water was present. Haruta et al. reported that the influence of water shifts from being positive to detrimental with increasing concentration.[44] They found that, above 200 ppm, water suppressed the CO oxidation activity of Au/TiO_2. There was a conspicuous decline in CO conversion with aging, which is expected to result from the sintering of gold during the high-temperature treatment.[45,46] Figure 6b hypothetically compares the CO_2 production from decomposition of formic acid with the oxidation of isoconcentrations of CO (650 ppm each) over the four catalysts under identical feed conditions ($W/F = 1.6 \times 10^{-4}$ g s cm^{-3}). At 300 °C, close to 100% CO_2 yield was obtained from formic acid decomposition over both the fresh and aged base-modified catalysts, while the CO conversion under identical conditions was only 18% and 10%, respectively. The unmodified catalyst exhibited 80% CO_2 yield from formic acid, while converting 11% CO. The acid-modified catalyst produced 54% CO_2 from formic acid decomposition and

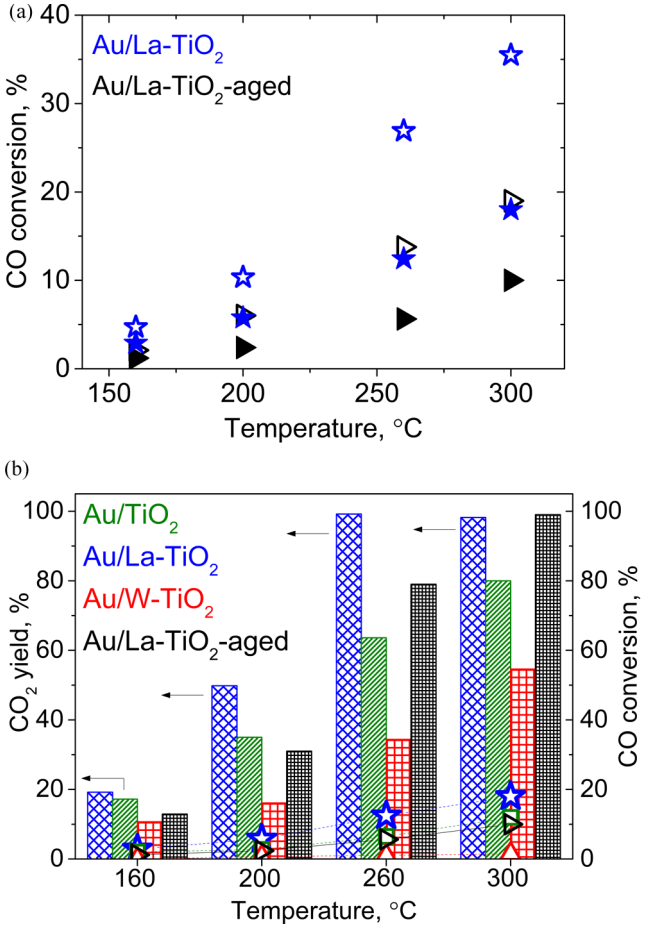

Figure 6. (a) Oxidation of 650 ppm of CO (gas phase) over $Au/La\text{-}TiO_2$ and $Au/La\text{-}TiO_2$-aged in the presence (filled symbols) and absence of water (open symbols). (b) Comparison of CO_2 produced from formic acid decomposition (bars) and gas-phase CO oxidation (scatters) as a function of temperature over Au/TiO_2, $Au/W\text{-}TiO_2$, $Au/La\text{-}TiO_2$, and $Au/La\text{-}TiO_2$-aged using 650 ppm formic acid and 650 ppm of CO at $W/F = 1.6 \times 10^{-4}$ g s cm^{-3}.

showed close to negligible conversion for CO oxidation. At 160 °C, there was no CO conversion over any of the catalysts. At the same temperature, Au/TiO_2, $Au/La\text{-}TiO_2$, and $Au/La\text{-}TiO_2$-aged produced 17%, 19%, and 13% CO_2, respectively, while $Au/W\text{-}TiO_2$ yielded 10% CO_2. Since the CO conversion is significantly lower or negligible in comparison to the total CO_2 produced from formic acid decomposition over all the catalysts under the investigated conditions, there must exist an independent pathway for CO_2 formation directly from formic acid that precludes CO formation and its subsequent oxidation. Therefore, it can be ascertained that base modification selectively promotes this direct formic acid oxidation pathway responsible for CO_2 formation without significantly affecting the oxidizing power of the catalyst.

Figure 7 illustrates the relative percentage increase in the pseudo-first-order mass-based rate constants for formic acid decomposition upon introduction of a stoichiometric amount of ammonia as a function of temperature over Au/TiO_2, $Au/La\text{-}TiO_2$, $Au/W\text{-}TiO_2$, and $Au/La\text{-}TiO_2$-aged. Au/TiO_2 exhibited the most pronounced effect of ammonia, followed by the base- and acid-modified catalysts. Aging did not alter the effect of ammonia. At 160 °C, in the presence of 1 molar equiv of ammonia, the formic acid decomposition rate underwent

DOI: 10.1021/acscatal.5b01057
ACS Catal. 2015, 5, 4772−4782

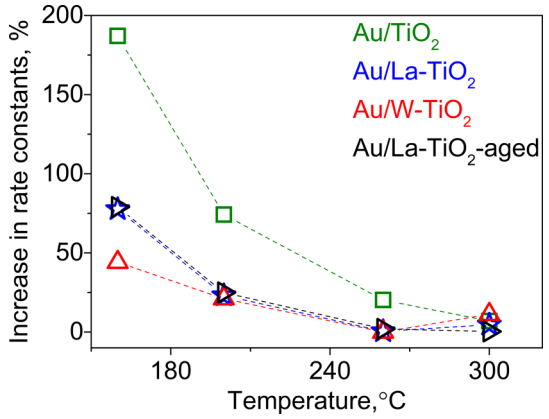

Figure 7. Effect of stoichiometric amount of ammonia on the formic acid decomposition rate constants over Au/TiO_2, $Au/W\text{-}TiO_2$, $Au/La\text{-}TiO_2$, and $Au/La\text{-}TiO_2$-aged at $W/F = 2.4 \times 10^{-5}$ g s cm^{-3}.

close to a 190% increase over the unmodified catalyst, while the base- and acid-modified catalysts showed ∼80% and 45% increases, respectively. At 200 °C, the extent of enhancement decreased to 74%, ∼23%, and 21% over the unmodified and base- and acid-modified catalysts, respectively. At 300 °C, the effect of ammonia on formic acid decomposition was negligible over the three catalysts. Dumesic and co-workers found that modification of alumina by lanthanum caused a decrease in the initial heat of ammonia adsorption by reducing the number of acid sites and simultaneously increasing the number of basic sites whose strength increased with increasing lanthanum loading.[47] The lower extent of ammonia-induced increase in rates over the base-modified catalysts can be rationally attributed to a lower level of interaction between ammonia and the basic surface of the catalysts. Even though the trend associated with the acid-modified catalyst appears counter-intuitive at first sight, it can be easily explained by taking into account the acidity of $Au/W\text{-}TiO_2$, which is likely to result in very high ammonia coverages.[48] It can be speculated that this would in turn be detrimental, causing unfavorable competition with formic acid, leading to the lowest degree of enhancement in comparison to unmodified and base-modified catalysts.

3.3. Formic Acid Reaction Orders and Activation Energy. To analyze the interaction between formic acid and the catalyst surface, experiments determining the apparent reaction orders were conducted using a wide range of formic acid concentrations (50−2500 ppm). Table 1 gives the kinetic orders for formic acid at 300 and 200 °C on Au/TiO_2, $Au/La\text{-}TiO_2$, $Au/W\text{-}TiO_2$, and $Au/La\text{-}TiO_2$-aged. On all of the catalysts, a negative order for formic acid, suggesting surface poisoning, was observed. Moreover, the order tended to be more negative at low temperature than at high temperature, which arises from an increased surface coverage of adsorbed formic acid species at low temperature, while a lower coverage may be favored at high temperature. Aging did not affect the reaction order for formic acid. The base-modified catalysts exhibited more negative orders for formic acid at both low and high temperatures than the unmodified and acid-modified catalysts. Cui et al. found that lanthanum modification of $Ni/\alpha\text{-}Al_2O_3$ lowered the reaction order for CO_2 from ∼0.6 to 0 for CO_2 re-forming of methane.[49] The ease of formation of

Table 1. Selectivity, Fractional Conversion, Apparent Activation Energy, Mass-Based Rate Constants, and Formic Acid Orders over Au/TiO_2, $Au/W\text{-}TiO_2$, $Au/La\text{-}TiO_2$, and $Au/La\text{-}TiO_2$-Aged Catalysts[a]

temp (°C)	k_{mass} (L g^{-1} s^{-1})[ba]	S_{CO_2} (%)[c]	S_{CO} (%)[c]	X_{CO_2} (%)[d]	X_{CO} (%)[d]	k_{CO_2} (L g^{-1} s^{-1})[e]	k_{CO} (L g^{-1} s^{-1})[e]	$E_{a,app}$ (±2.0 kJ mol^{-1}) formic acid	$E_{a,app}$ (±2.0 kJ mol^{-1}) AmFo	formic acid order (±0.1)
					Au/TiO_2					
300	26.8	81.0	19.0	0.81	0.19	21.7	5.1	33.7	14	−0.5[g]
260	13.1	93.0	7.0	0.93	0.07	12.2	0.9			
200	4.7	100.0	0.0	1.00	0.00	4.7	0			−0.7[g]
160	2.2	100.0	0.0	1.00	0.00	2.2	0			
					$Au/La\text{-}TiO_2$					
300	90.3	97.8	2.2	0.98	0.02	88.5	1.8	48.2, 34.9[f]	37.6	−0.7,[g] −0.4[h]
260	41.4	99.1	0.9	0.99	0.01	40.9	0.4			
200	9.4	100.0	0.0	1.00	0.00	9.4	0			−0.9,[g] −0.7[h]
160	3.4	100.0	0.0	1.00	0.00	3.4	0			
					$Au/W\text{-}TiO_2$					
300	10.1	70.7	29.3	0.71	0.29	7.1	2.9	30.1	22.5	−0.3[g]
260	4.5	89.3	10.7	0.89	0.11	4.0	0.5			
200	1.6	100.0	0.0	1.00	0.00	1.6	0			−0.5[g]
160	0.9	100.0	0.0	1.00	0.00	0.9	0			
					$Au/La\text{-}TiO_2$-aged					
300	37.5	98.2	2.1	0.98	0.02	36.7	0.8	48.9, 34.4[f]	37.5	−0.6,[g] −0.4[h]
260	22.5	99.6	0.6	1.00	0.00	22.5	0			
200	4.3	100.0	0	1.00	0.00	4.3	0			−0.9,[g] −0.7[h]
160	1.9	100.0	0	1.00	0.00	1.9	0			

[a]All values were determined using $W/F = 2.4 \times 10^{-5}$ g s cm^{-3}, 750 L h^{-1} total flow with 10 vol % oxygen, 5 vol % water, and 85 vol % nitrogen to simulate exhaust gas composition, and 650 ppm formic acid unless otherwise mentioned. [ba]Total mass-based pseudo-first-order rate constant. [c]Selectivity. [d]Fractional formic acid conversion. [e]Mass-based pseudo-first-order rate constant. [f]Determined using low concentration of formic acid (120 ppm). [g]Determined using formic acid concentrations in the range 600−2200 ppm, with a step size of ∼300 ppm. [h]Determined using formic acid concentrations in the range 50−150 ppm, with a step size of 30 ppm.

DOI: 10.1021/acscatal.5b01057
ACS Catal. 2015, 5, 4772−4782

$La_2O_2CO_3$ contributed to the decrease of the CO_2 order. Similarly, Leveles et al. observed negative orders as low as −0.5 for CO_2 for oxidative dehydrogenation of propane owing to the high basicity of lithium-promoted magnesia catalysts.[50] In our system, as demonstrated by in situ DRIFT, there exists a higher affinity of formic acid for the highly basic catalyst surface, which correlates with the most negative reaction orders for formic acid in the case of the lanthanum-modified catalysts. At 200 °C, the base-modified catalysts exhibited formic acid orders as low as −1.0, which signifies extensive blockage of the catalytic sites. Hence, the strong binding and arrested desorption of formic acid species can explain the relatively lower performance of the base-modified catalysts at temperatures ≤200 °C.

Figure 8 (shaded area) compares the apparent activation energy ($E_{a,app}$, kJ mol^{-1}) and pre-exponential factor (A) for

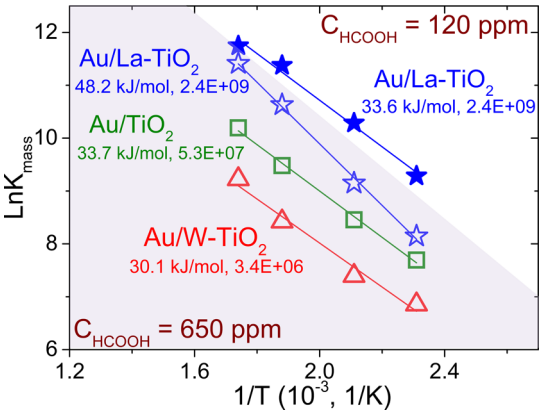

Figure 8. Arrhenius plots for Au/TiO_2, $Au/W\text{-}TiO_2$, and $Au/La\text{-}TiO_2$ for formic acid decomposition (shaded area, 650 ppm formic acid; nonshaded area, 120 ppm formic acid) at $W/F = 2.4 \times 10^{-5}$ g s cm^{-3}.

formic acid decomposition to CO_2 over the three catalysts using formic acid as the precursor. The unshaded area of the plot represents the Arrhenius curves determined using 650 ppm of formic acid. The unmodified and acid-modified catalysts exhibited similar $E_{a,app}$ values in the range of 30−35 kJ mol^{-1} for formic acid decomposition, while the base-modified catalyst showed a higher $E_{a,app}$ of ∼50 kJ mol^{-1}. Concomitantly, lanthanum modification increased A by 2 orders of magnitude in comparison to the unmodified catalyst. This sort of compensation is commonly observed when the surface concentration of the reactant species changes with temperature,[51,52] which is the case, as confirmed by the more negative formic acid order at lower temperature. To assess the influence of the formic acid adsorption enthalpy on the $E_{a,app}$ value of the lanthanum-modified catalyst, a decomposition experiment was performed using lower formic acid concentration (120 ppm). The resulting $E_{a,app}$ value was ∼15 kJ mol^{-1} lower than the $E_{a,app}$ value obtained at higher formic acid concentration (650 ppm), while A remained unchanged (nonshaded area). Such a contribution of the enthalpy of formic acid adsorption to $E_{a,app}$ was reported by Fein and Wachs for formic acid oxidation over metal oxides.[53] This supports our findings on the kinetic orders for formic acid, which assume smaller negative values at lower concentrations of formic acid (Table 1). Hence, a part of the thermal energy is utilized to desorb the strongly adsorbed formate species, resulting in an apparent activation energy higher than the intrinsic value.[51] The aged base-modified catalyst exhibited an $E_{a,app}$ value identical with that of $Au/La\text{-}TiO_2$, while A decreased by an order of magnitude (Table 1).

Table 1 gives the $E_{a,app}$ values for formic acid decomposition over Au/TiO_2, $Au/La\text{-}TiO_2$, $Au/W\text{-}TiO_2$, and $Au/La\text{-}TiO_2$-aged catalysts in the temperature in the range of 160−260 °C when AmFo was used as the precursor. At 300 °C there was no effect of ammonia on formic acid decomposition (Figure 4a). In the case of the unmodified catalyst, the activation energy was lowered by more than 50% in the presence of stoichiometric amounts of ammonia. The acid- and base-modified catalysts did not display such a pronounced ammonia-induced effect on the activation energies. This substantiates the occurrence of an optimum favorable interaction with ammonia over the unmodified catalyst, as demonstrated by the trend in the relative magnitudes of the ammonia-induced increase in the rate constants over the four catalysts (Figure 7). Table 1 also gives the product selectivity, fractional conversion, and mass-based pseudo-first-order rate constants derived from formic acid decomposition in the temperature range of 160−300 °C. X_{CO_2} and X_{CO} represent the fractional formic acid conversion, while k_{CO_2} and k_{CO} denote the pseudo-first-order mass-based rate constants relevant for the formation of the respective products. At 300 °C, $Au/La\text{-}TiO_2$ exhibited k_{CO_2} and k_{CO} values of ∼90 and ∼2 L g s^{-1}, respectively, which are ∼4-fold greater and ∼2.5-fold less than the corresponding values obtained over Au/TiO_2. On the other hand, tungsten modification reduced k_{CO_2} by 3-fold, while k_{CO} remained at more than 50% of the corresponding value obtained over Au/TiO_2. This corresponded to fractional formic acid conversion to CO of 19%, 2%, and 29% over Au/TiO_2, $Au/La\text{-}TiO_2$, and $Au/W\text{-}TiO_2$, respectively. At 260 °C, formic acid decomposed to CO_2 with a selectivity of >99% and 93% over the base-modified catalysts and Au/TiO_2, respectively, while the acid-modified catalyst showed only 89% CO_2 selectivity. At temperatures ≥260 °C, the $Au/La\text{-}TiO_2$-aged still exhibited a close to 2-fold higher k_{CO_2} value in comparison to Au/TiO_2. Concomitantly, k_{CO} varied from only 0.8 L g^{-1} s^{-1} at 300 °C to ∼0 at 260 °C over $Au/La\text{-}TiO_2$-aged, which are significantly lower than the corresponding values over Au/TiO_2. In agreement with the higher $E_{a,app}$ values of the base-modified catalysts, the low-temperature decomposition activities (k_{CO_2}) of $Au/La\text{-}TiO_2$ and $Au/La\text{-}TiO_2$-aged at 160 °C were 3.3 and 1.9 L g^{-1} s^{-1}, respectively, which is similar to that of Au/TiO_2 (2.1 L g^{-1} s^{-1}). Overall, the rates on $Au/La\text{-}TiO_2$-aged underwent close to 0.5-fold decrease upon 5 h of thermal treatment at 600 °C, while the selectivity and the fractional conversion remained unchanged in comparison to the parent base-modified catalyst.

3.4. Activity of the Supports in the Absence of Gold.

To delineate the influence of gold, formic acid decomposition experiments were conducted over the bare supports. Similar to the decomposition selectivity of bare titania,[9] CO was the only product from formic acid decomposition over the acid- and base-modified supports. Figure 9 compares the CO yield obtained from formic acid decomposition over TiO_2, $La\text{-}TiO_2$, $W\text{-}TiO_2$, and $La\text{-}TiO_2$-aged at $W/F = 1.6 \times 10^{-4}$ g s cm^{-3}. The aged base-modified support did not exhibit any significant change in the formic acid decomposition activity in comparison to the fresh $La\text{-}TiO_2$. In contrast to the activity trend in the gold catalysts, the supports displayed increasing activity with decreasing basicity, suggesting that a different mechanism operates in the absence of gold. At 300 °C, $W\text{-}TiO_2$ and TiO_2

DOI: 10.1021/acscatal.5b01057
ACS Catal. 2015, 5, 4772−4782

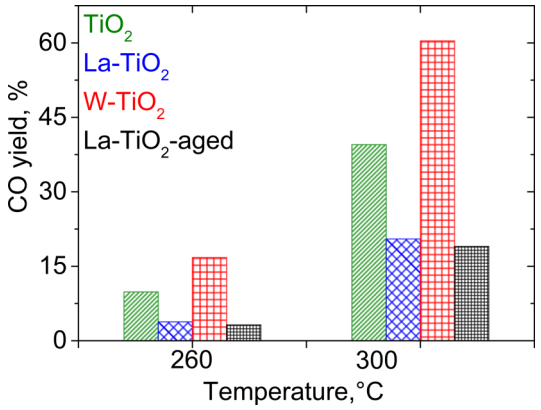

Figure 9. Comparison of CO yield from formic acid decomposition over TiO_2, W-TiO_2, La-TiO_2, and La-TiO_2-aged supports at $W/F = 1.6 \times 10^{-4}$ g s cm^{-3}.

produced 60% CO and 40% CO, respectively, while the base-modified supports yielded only ~20% CO. At 260 °C, the base-modified supports (both fresh and aged) produced less than 25% CO in comparison to W-TiO_2. Hence, the observed low CO selectivity of Au/La-TiO_2 may be associated with the inherent low formic acid decomposition activity of the support. Reports on such an "acid-promoted dehydration mechanism" to form CO from formic acid are prevalent in the literature.[38,54] Ai has proposed a switchover of the formic acid decomposition pathway from oxidative dehydrogenation forming CO_2 to a dehydration mechanism yielding CO with increasing acidity of the catalyst, further adding that an increased acidity correlated with increasing dehydration activity.[54] At temperatures ≤200 °C, we observed negligible CO formation over all the supports, which correlates with negligible CO yield observed over the gold catalysts at these temperatures. Furthermore, it is clear that, even in the case of the best-performing catalyst (Au/La-TiO_2), the presence of gold is indispensable to realize high activity, without which the support is virtually inactive for formic acid decomposition.

3.5. Effect of Increased Gold Loading. Since bare supports selectively decompose formic acid to CO, the pathway responsible for CO_2 production from formic acid must be associated with the presence of gold. Hence, an increase in the gold loading should tantamount to increased CO_2 formation. Figure 10 traces the evolution of CO_2 and CO yield derived from formic acid decomposition as a function of gold loading at $W/F = 4.9 \times 10^{-5}$ g s cm^{-3}. A systematic increase in the CO_2/CO ratio was witnessed with increasing gold content over titania. At 300 °C, the CO_2 yield increased from 39% to 98% upon a 4-fold increase in the gold content, while the CO yield dropped from 8% to 2%. At 200 °C, no CO production occurred over any of the catalysts; however, the CO_2 production experienced a 4-fold increase from 12% to 48%. These results in conjunction with the 100% CO selectivity evidenced over bare supports imply that the active sites for CO_2 production must reside either on gold or at the interface between the gold particles and the support. The number of these sites increases with gold loading, which in turn manifests itself in the form of higher CO_2 production rates. Retrospectively, the CO_2/CO ratios of the base-modified catalysts with 0.5 wt % gold loading are closely similar to those of the unmodified catalysts with 2 wt % gold, suggesting that lanthanum modification preferentially increases the active sites associated with CO_2 production, while those forming CO remain disfavored.

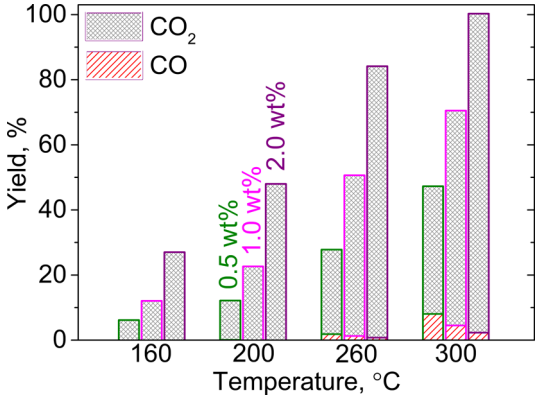

Figure 10. Effect of gold loading on the product distribution during formic acid decomposition over the unmodified support as a function of temperature at $W/F = 4.9 \times 10^{-5}$ g s cm^{-3}.

3.6. Implications on the Mechanism. Lanthanum modification of titania resulted in two phenomena: stabilization of smaller gold particles and a substantial increase in the support basicity. Thermal-induced gold particle growth enabled us to disentangle the two effects and compare the catalysts at identical gold loadings and gold particle sizes but on different supports. While the CO oxidation activity, which is irrelevant to our decomposition mechanism, showed sensitivity to the gold particle size, the observed trend in the selectivity of formic acid decomposition toward CO_2 can be exclusively indexed as a consequence of basicity. The formic acid orders in conjunction with the in situ DRIFT studies reveal that the catalytic activity is significantly influenced by formic acid adsorption, which in turn is greatly augmented upon base modification. High formic acid coverages reflected in the crossing of the Arrhenius plots. This justifies the significantly higher activities of the lanthanum-modified catalysts in comparison to the unmodified catalysts at higher temperatures (≥260 °C). The rate of CO_2 production increased proportionally with gold loading, with gold being indispensable for selective formic acid decomposition to CO_2. Scheme 1 outlines the following mechanistic insights: formate is formed as a relevant reactive intermediate upon formic acid adsorption on both the unmodified and lanthanum-modified catalysts. The formate density is greatly enhanced upon lanthanum modification, which characterizes the higher rates for CO_2 production. The high formic acid coverages obviate the

Scheme 1. Preliminary Mechanistic Description of Formic Acid Decomposition over the Unmodified and Lanthanum-Modified Catalysts

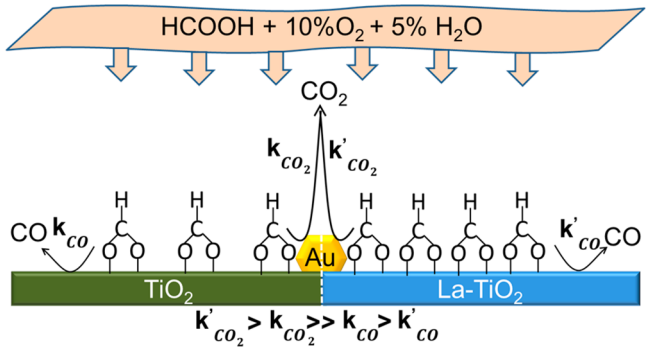

DOI: 10.1021/acscatal.5b01057
ACS Catal. 2015, 5, 4772−4782

step of dissociative chemisorption of formic acid as the rate-determining step (rds), meaning that the next step(s) involving the oxidative dehydrogenation of formate to CO_2 is likely to be the rds.[39] In the absence of gold, the formates selectively decompose to CO over the bare supports, whose rates follow an opposite trend in relation to the support basicity.

3.7. Outlook on the Use of AmFo as an Alternative Reducing Agent. Applications reporting the use of AmFo as an additive to aqueous urea solution have demonstrated the existence of dual advantages in the form of freezing point depression and increased ammonia storage capacity.[55−58] Formulations containing AmFo and urea have been commercially employed, either under the name Denoxium or, in Canada, the USA, and Mexico, under the name TerraCairPlus, due to a license agreement between Denoxium owner Kemira Oyj with Terra Environmental Technologies Inc.[59] Taking into account the serious problems associated with the use of urea[3,4] and the aformentioned benefits of AmFo, the latter by itself strikes as a promising candidate. AmFo thermolyzes in the hot exhaust to form ammonia and formic acid.[9] While ammonia can be desirably consumed by the SCR reaction, there is a need to rapidly decompose the highly corrosive and reactive formic acid. Our study, which is in line with the alternative exhaust gas aftertreatment system conceived by Hammer et al. and Gerhart et al.,[60,61] envisages the independent operation of the gold catalyst in a separate side stream reactor built in parallel to the SCR compartment. This way, complete and selective decomposition of ammonium formate to ammonia and CO_2 can be achieved, circumventing the problems of side product formation and enabling the provision of a clean stream of ammonia upstream of the SCR catalyst, thus resulting in enhanced $DeNO_x$ efficiency.

4. CONCLUSION

The activity of Au/TiO_2 for AmFo and formic acid decomposition could be significantly improved by translating the previously observed promotional effect of the basic gas-phase reactant (ammonia) into a catalytic effect by modification of the support with a basic additive. Such a catalyst design for formic acid decomposition in the context of application in SCR is unique. Regardless of the high activity, the base-modified catalysts remained selective against ammonia oxidation, which is a critical criterion for SCR applications. The lanthanum modification of titania affected both the gold particle size and the support basicity. The resulting higher activity of the lanthanum-modified catalysts was characterized by significantly higher formic acid coverages under the reaction conditions. The observations in this study can be qualitatively explained with a mechanism where the density of formates, which are relevant reaction intermediates, is greatly increased upon base modification. CO_2 production increased systematically with increasing gold loading, while the bare supports exclusively produced CO from formic acid decomposition, implying that the active site must be associated with the gold. It is speculated that the introduction of lanthanum culminates in the formation of a new type of site that rapidly and selectively decomposes formic acid to CO_2. On the other hand, acid modification with tungsten rendered the catalyst less active and less selective for CO_2 production.

AUTHOR INFORMATION

Corresponding Authors

*J.A.v.B.: e-mail, jeroen.vanbokhoven@chem.ethz.ch; tel, +41 44 632 5542.

*O.K.: e-mail, oliver.kroecher@psi.ch; tel, +41 56 310 2066.

Notes

The authors declare no competing financial interest.

ACKNOWLEDGMENTS

Financial support from the Swiss National Science Foundation (SNF, project number 200021_143430/1) is gratefully acknowledged. We extend our gratitude to Dr. Mohammed Tarik for aiding us with ICP-OES and to Dr. Frank Krumeich (ETH) for the microscopy work.

REFERENCES

(1) Johnson, T. V. *Int. J. Engine Res.* **2009**, *10* (5), 275−285.

(2) Trichard, J. M. In *Past and Present in DeNOx Catalysis From Molecular Modelling to Chemical Engineering*; Elsevier: Amsterdam, 2007; Catalysis Vol. *171*, pp 211−233.

(3) Kröcher, O.; Elsener, M.; Jacob, E. *Appl. Catal., B* **2009**, *88* (1−2), 66−82.

(4) Eichelbaum, M.; Siemer, A. B.; Farrauto, R. J.; Castaldi, M. J. *Appl. Catal., B* **2010**, *97* (1−2), 98−107.

(5) Kröcher, O.; Daniel, P. Ammonia generator converting liquid ammonia precursor solutions to gaseous ammonia for denox-applications using selective catalytic reduction of nitrogen oxides. WO2012104205 (A1), February 4, 2011.

(6) Bernhard, A.; Peitz, D.; Elsener, M.; Kröcher, O. *Top. Catal.* **2013**, *56* (1−8), 130−133.

(7) Eichelbaum, M.; Farrauto, R. J.; Castaldi, M. J. *Appl. Catal., B* **2010**, *97* (1−2), 90−97.

(8) Lundström, A.; Snelling, T.; Morsing, P.; Gabrielsson, P.; Senar, E.; Olsson, L. *Appl. Catal., B* **2011**, *106* (3−4), 273−279.

(9) Sridhar, M.; Bokhoven, J. A. van; Kröcher, O. *Appl. Catal., A* **2014**, *486*, 219−229.

(10) Sridhar, M.; Peitz, D.; van Bokhoven, J.; Kröcher, O. *Chem. Commun.* **2014**, *50*, 6998.

(11) Zhu, X.; Shen, M.; Lobban, L. L.; Mallinson, R. G. *J. Catal.* **2011**, *278* (1), 123−132.

(12) Evin, H.; Jacobs, G.; Ruiz-Martinez, J.; Graham, U.; Dozier, A.; Thomas, G.; Davis, B. *Catal. Lett.* **2008**, *122* (1−2), 9−19.

(13) Zhai, Y.; Pierre, D.; Si, R.; Deng, W.; Ferrin, P.; Nilekar, A. U.; Peng, G.; Herron, J. A.; Bell, D. C.; Saltsburg, H.; Mavrikakis, M.; Flytzani-Stephanopoulos, M. *Science* **2010**, *329* (5999), 1633−1636.

(14) Panagiotopoulou, P.; Kondarides, D. I. *J. Catal.* **2008**, *260* (1), 141−149.

(15) Pazmiño, J. H.; Shekhar, M.; Damion Williams, W.; Cem Akatay, M.; Miller, J. T.; Nicholas Delgass, W.; Ribeiro, F. H. *J. Catal.* **2012**, *286* (0), 279−286.

(16) Bulushev, D. A.; Jia, L.; Beloshapkin, S.; Ross, J. R. H. *Chem. Commun.* **2012**, *48* (35), 4184−4186.

(17) Zhu, J.; Figueiredo, J. L.; Faria, J. L. *Catal. Commun.* **2008**, *9* (14), 2395−2397.

(18) Jiang, X.; Zhou, R.; Pan, P.; Zhu, B.; Yuan, X.; Zheng, X. *Appl. Catal., A* **1997**, *150* (1), 131−141.

(19) Borer, A. L.; Prins, R. *J. Catal.* **1993**, *144* (2), 439−451.

(20) Devadas, M.; Kröcher, O.; Wokaun, A. xx. *React. Kinet. Catal. Lett.* **2005**, *86* (2), 347−354.

(21) Peitz, D.; Bernhard, a; Elsener, M.; Kröcher, O. *Rev. Sci. Instrum.* **2011**, *82* (8), 084101.

(22) Joshi, S. Y.; Harold, M. P.; Balakotaiah, V. *Chem. Eng. Sci.* **2010**, *65* (5), 1729−1747.

(23) Hayes, R. E.; Liu, B.; Moxom, R.; Votsmeier, M. *Chem. Eng. Sci.* **2004**, *59* (15), 3169−3181.

(24) Bernhard, A. M.; Peitz, D.; Elsener, M.; Schildhauer, T.; Krocher, O. *Catal. Sci. Technol.* **2013**, *3* (4), 942−951.

DOI: 10.1021/acscatal.5b01057
ACS Catal. 2015, 5, 4772−4782

(25) Gibson, L. T.; Cooksey, B. G.; Littlejohn, D.; Tennent, N. H. *Anal. Chim. Acta* **1997**, *341* (1), 1−10.
(26) Kleemann, M.; Elsener, M.; Koebel, M.; Wokaun, A. *Ind. Eng. Chem. Res.* **2000**, *39* (11), 4120−4126.
(27) Peitz, D.; Bernhard, A.; Elsener, M.; Kröcher, O. *Top. Catal.* **2013**, *56* (1−8), 19−22.
(28) Zhang, J.; Xu, Q.; Feng, Z.; Li, C. In *Environmentally Benign Photocatalysts SE-6*; Anpo, M., Kamat, P. V, Eds.; Springer: New York, 2010; Nanostructure Science and Technology, pp 153−184.
(29) Shastri, A. G.; Datye, A. K.; Schwank, J. *J. Catal.* **1984**, *87* (1), 265−275.
(30) Kim, D.-S.; Yang, J.-H.; Balaji, S.; Cho, H.-J.; Kim, M.-K.; Kang, D.-U.; Djaoued, Y.; Kwon, Y.-U. *CrystEngComm* **2009**, *11* (8), 1621−1629.
(31) Ramis, G.; Busca, G.; Cristiani, C.; Lietti, L.; Forzatti, P.; Bregani, F. *Langmuir* **1992**, *8* (7), 1744−1749.
(32) Busca, G.; Lorenzelli, V. *Mater. Chem.* **1982**, *7* (1), 89−126.
(33) Collins, S. E.; Baltanás, M. A.; Bonivardi, A. L. *J. Phys. Chem. B* **2006**, *110* (11), 5498−5507.
(34) Li, C.; Sakata, Y.; Arai, T.; Domen, K.; Maruya, K.; Onishi, T. *J. Chem. Soc., Faraday Trans. 1* **1989**, *85* (4), 929−943.
(35) Morterra, C.; Chiorino, A.; Boccuzzi, F.; Fisicaro, E. *Z. Phys. Chem.* **1981**, *124* (2), 211−222.
(36) Busca, G.; Lamotte, J.; Lavalley, J. C.; Lorenzelli, V. *J. Am. Chem. Soc.* **1987**, *109* (17), 5197−5202.
(37) Liao, L.-F.; Wu, W.-C.; Chen, C.-Y.; Lin, J.-L. *J. Phys. Chem. B* **2001**, *105* (32), 7678−7685.
(38) Criado, J. M.; Gonzalez, F.; Trillo, J. M. *J. Catal.* **1971**, *23* (1), 11−18.
(39) Samjeské, G.; Osawa, M. *Angew. Chem.* **2005**, *117* (35), 5840−5844.
(40) Ma, Z.; Yin, H.; Dai, S. *Catal. Lett.* **2010**, *136* (1−2), 83−91.
(41) Yu, J.; Wu, G.; Lu, G.; Mao, D.; Guo, Y. *RSC Adv.* **2014**, *4* (33), 16985−16991.
(42) Chen, Y.-X.; Heinen, M.; Jusys, Z.; Behm, R. J. *Langmuir* **2006**, *22* (25), 10399−10408.
(43) Neurock, M.; Janik, M.; Wieckowski, A. *Faraday Discuss.* **2009**, *140*, 363−378.
(44) Date, M.; Haruta, M. *J. Catal.* **2001**, *201* (2), 221−224.
(45) Grisel, R.; Weststrate, K.-J.; Gluhoi, A.; Nieuwenhuys, B. *Gold Bull.* **2002**, *35* (2), 39−45.
(46) Mavrikakis, M.; Stoltze, P.; Nørskov, J. K. *Catal. Lett.* **2000**, *64* (2−4), 101−106.
(47) Shen, J.; Cortright, R. D.; Chen, Y.; Dumesic, J. A. *J. Phys. Chem.* **1994**, *98* (33), 8067−8073.
(48) Kleemann, M.; Elsener, M.; Koebel, M.; Wokaun, A. *Appl. Catal., B* **2000**, *27* (4), 231−242.
(49) Cui, Y.; Zhang, H.; Xu, H.; Li, W. *Appl. Catal., A* **2007**, *331* (0), 60−69.
(50) Leveles, L.; Seshan, K.; Lercher, J. A.; Lefferts, L. *J. Catal.* **2003**, *218* (2), 296−306.
(51) Bond, G. C. *Catal. Rev.: Sci. Eng.* **2008**, *50* (4), 532−567.
(52) Bond, G. C.; Keane, M. A.; Kral, H.; Lercher, J. A. *Catal. Rev.: Sci. Eng.* **2000**, *42* (3), 323−383.
(53) Fein, D. E.; Wachs, I. E. *J. Catal.* **2002**, *210* (2), 241−254.
(54) Ai, M. *J. Catal.* **1977**, *50* (2), 291−300.
(55) Solla, A.; Westerholm, M.; Söderström, C.; Tormonen, K.; Härmä, T.; Nissinen, T.; Kukkonen, J. *Effect of ammonium formate and mixtures of urea and ammonium formate on low temperature activity of SCR systems*; SAE: Warrendale, PA, 2005; SAE Technical Paper.
(56) Nissinen, T.; Kukkonen, J. Catalytic process for reducing nitrogen oxides in flue gases and reducing agent composition. FI2004000057, September 29, 2009.
(57) Armin, M.; Wahl, T.; Ulrich, A.; Brenner, F.; Bareis, M.; Horst, H. Method and apparatus for selective catalytic NOx reduction. WO1999001205A1, February 21, 2013.
(58) Koebel, M.; Elsener, M. *Ind. Eng. Chem. Res.* **1998**, *37* (10), 3864−3868.
(59) Kemira and Terra Environmental Technologies Inc. signed license agreement of Kemira's Denoxium; http://www.kemira.com/en/media/whatsup/Pages/KemiraTerraDenoxium.aspx.
(60) Hammer, B.; Krimmer, H. P.; Schulz, B.; Jacob, E. Use of aqueous guanidinium formate solutions for the selective catalytic reduction of nitrogen oxides in exhaust gases of vehicles. WO2008077587-A1, July 3, 2008.
(61) Gerhart, C.; Krimmer, H.-P.; Hammer, B.; Schulz, B.; Kröcher, O.; Paul, S. I.; Peitz, D.; Paul, S. I.; Sattelmayer, T.; Toshev, P.; Wachtmeister, G.; Heubuch, A.; Jacob, E. *SAE Int. J. Engines* **2012**, *5* (3), 938−946.

DOI: 10.1021/acscatal.5b01057
ACS Catal. 2015, 5, 4772−4782